

RESEARCH ARTICLE

Genetics of Microstructure of the Corpus Callosum in Older Adults

Sri C. Kanchibhotla¹, Karen A. Mather¹, Anbupalam Thalamuthu¹, Lin Zhuang¹, Peter R. Schofield^{2,3}, John B. J. Kwok^{2,3}, David Ames^{4,5}, Margaret J. Wright⁶, Julian N. Trollor^{1,7}, Wei Wen^{1,8}, Perminder S. Sachdev^{1,8*}

1. Centre for Healthy Brain Ageing, School of Psychiatry, University of New South Wales, Sydney, Australia, 2. Neuroscience Research Australia, Sydney, Australia, 3. School of Medical Science, University of New South Wales, Sydney, Australia, 4. National Ageing Research Institute, Royal Melbourne Hospital, Melbourne, Australia, 5. Academic Unit for Psychiatry of Old Age, University of Melbourne, Melbourne, Australia, 6. Queensland Institute Medical Research, Berghofer Medical Research Institute, Brisbane, Australia, 7. Department Developmental Disability Neuropsychiatry, University of New South Wales, Sydney, Australia, 8. Neuropsychiatric Institute, The Prince of Wales Hospital, Sydney, Australia

*p.sachdev@unsw.edu.au



 OPEN ACCESS

Citation: Kanchibhotla SC, Mather KA, Thalamuthu A, Zhuang L, Schofield PR, et al. (2014) Genetics of Microstructure of the Corpus Callosum in Older Adults. PLoS ONE 9(12): e113181. doi:10.1371/journal.pone.0113181

Editor: William Barendse, CSIRO, Australia

Received: May 14, 2014

Accepted: October 21, 2014

Published: December 16, 2014

Copyright: © 2014 Kanchibhotla et al. This is an open-access article distributed under the terms of the [Creative Commons Attribution License](http://creativecommons.org/licenses/by/4.0/), which permits unrestricted use, distribution, and reproduction in any medium, provided the original author and source are credited.

Data Availability: The authors confirm that, for approved reasons, some access restrictions apply to the data underlying the findings. De-identified data will be made available to interested researchers upon request, which should be submitted to the Older Australian Twins Governance Committee, Centre for Healthy Brain Ageing, UNSW Australia (<http://cheba.unsw.edu.au/project/older-australian-twins-study>).

Funding: OATS is supported by the NHMRC/ Australian Research Council Strategic Award 401162 and NHMRC Project Grant 1045325. OATS was facilitated through access to the Australian Twin Registry, a national research resource supported by the NHMRC Enabling Grant 310667, administered by the University of Melbourne. Sri Chandana Kanchibhotla is supported by a scholarship from the Dementia Collaborative Research Centre (DCRC). Karen Mather is supported by an Alzheimer's Australia Dementia Research Foundation Postdoctoral Fellowship and the NHMRC Capacity Building Grant 568940. The funders had no role in study design, data collection and analysis, decision to publish, or preparation of the manuscript.

Competing Interests: The authors have declared that no competing interests exist.

Abstract

The current study sought to examine the relative influence of genetic and environmental factors on corpus callosum (CC) microstructure in a community sample of older adult twins. Analyses were undertaken in 284 healthy older twins (66% female; 79 MZ and 63 DZ pairs) from the Older Australian Twins Study. The average age of the sample was 69.82 (SD=4.76) years. Brain imaging scans were collected and DTI measures were estimated for the whole CC as well as its five subregions. Parcellation of the CC was performed using Analyze. In addition, white matter lesion (WMLs) burden was estimated. Heritability and genetic correlation analyses were undertaken using the SOLAR software package. Age, sex, scanner, handedness and blood pressure were considered as covariates. Heritability (h^2) analysis for the DTI metrics of whole CC, indicated significant h^2 for fractional anisotropy (FA) ($h^2=0.56$; $p=2.89 \times 10^{-10}$), mean diffusivity (MD) ($h^2=0.52$; $p=0.30 \times 10^{-6}$), radial diffusivity (RD) ($h^2=0.49$; $p=0.2 \times 10^{-6}$) and axial diffusivity (AD) ($h^2=0.37$; $p=8.15 \times 10^{-5}$). We also performed bivariate genetic correlation analyses between (i) whole CC DTI measures and (ii) whole CC DTI measures with total brain WML burden. Across the DTI measures for the whole CC, MD and RD shared 84% of the common genetic variance, followed by MD- AD (77%), FA - RD (52%), RD - AD (37%) and FA - MD (11%). For total WMLs, significant genetic correlations indicated that there was 19% shared common genetic variance with whole CC MD, followed by CC RD (17%), CC AD (16%) and CC FA (5%). Our findings suggest that the CC microstructure is under moderate genetic control. There was also evidence of shared genetic factors between the CC DTI measures.

In contrast, there was less shared genetic variance between WMLs and the CC DTI metrics, suggesting fewer common genetic variants.

Introduction

The corpus callosum (CC) is the largest white matter (WM) tract connecting the two cerebral hemispheres and contains more than 2×10^8 axons [1, 2]. The size and myelination of these fibres determine the time taken for inter-hemispheric transfer of information [3].

Diffusion tensor imaging (DTI) is used to study WM integrity, and it provides quantitative three-dimensional analyses of WM microstructure [4, 5]. Different DTI measures such as anisotropy (fractional anisotropy-FA) and diffusivity (mean diffusivity- MD; radial diffusivity- RD and axial diffusivity- AD) can be obtained, each of which is sensitive to different aspects of WM integrity, including levels of myelination (FA, RD), axonal density/diameter (FA), axonal damage or loss (AD) [6–10].

Ageing leads to macro and microstructural changes to fibres in the CC, affecting inter-hemispheric processing [11]. Although the number of fibres in the CC does not change from birth [12], their size, density [2] and composition (myelination) [12] varies with age [1]. For the CC, greater atrophy using DTI measures has been observed with increasing age in the anterior and mid-body regions compared to posterior regions [5, 13, 14].

Age-related changes in the CC [15, 16] have been associated with age-related cognitive impairment [17–19], reduced processing speed [20], bimanual motor decline [21] and neurodegenerative disease [22–25]. Moreover, the study of WM integrity measures in older individuals may help in the early diagnosis of disease such as Alzheimer's disease and mild cognitive impairment [26–28] and may serve as biomarkers to differentiate them at an early stage [29]. Hence, it is important to gain a better understanding of the role of genetic and environmental factors in age-related integrity of the CC. Further, studying the genetics of CC in older individuals may help to understand the aetiology of the age-related degeneration of CC and also clarify the relationship between its microstructure, function and disease.

Heritability studies provide evidence for the role of genes in WM integrity [30]. To date, however, the heritability of CC in older individuals has been reported in only two studies, one examining FA in older males only [31], while the other used an extended family study design [32]. In a small sample of older males ($n=64$), the heritability for FA of the CC splenium (67%) was found to be more than that of the genu (49%) [31]. However, in an extended family study ($n=467$), which included older adults (age range 19–85 yrs), heritability of FA across the lifespan for the genu was high (66%), with heritability values of FA for the body of CC and splenium ranging from 54–57%. Also, CC RD was reported to be heritable (37%),

but not AD [32]. The heritability of MD was not reported in either of these two studies. Therefore, more studies are required to examine heritability of all CC DTI measures using larger samples of older adults and including females.

One major consideration in the study of the CC is how best to divide it into sub regions (parcellation) it. Many of the previous reports only studied the whole CC as a single unit or divided it into two (genu & splenium) or three (genu, mid body& splenium) regions. However, the CC has no clear anatomical boundaries [1], and it varies highly in size and shape among individuals [12, 33–35]. The widely accepted Witelson's classification [36], and other geometric parcellation methods [37, 38], are not based on fibre composition and connections and may therefore not exactly reflect the functional regions of CC [39]. Although there are several other methods of parcellation [40–42], these methods are based on their connections to the target regions in the cortex, leading to inconsistent sub divisions of CC. Chao et al., [39] proposed parcellation of the CC based on high angular resolution diffusion imaging (HARDI) and the neural connections of CC with distinct cerebral areas, sub divided further based on differences in cell layers and structures. When using this method, the CC is parcellated based on its connections to distinct brain functional units. An added advantage is that HARDI can assist in resolving even lateral and crossing fibres. Hence, this probabilistic topographical method helps to better understand the fibre composition of the CC [39].

WM lesions (WMLs) are a marker of WM pathology and are commonly observed as hyperintense regions in T2-weighted or fluid attenuated inversion recovery (FLAIR) scans in older adults. WMLs are thought to reflect small vessel disease but their aetiology is incompletely understood [43, 44]. WMLs have moderate to high heritability and are influenced by both genetic and environmental factors [45]. Although, several studies reported an association of the development of these WMLs with WM integrity measures across several regions of the brain [46–48], it is unclear whether common genetic factors influence WMLs and age-related WM integrity measures. To date, there are no studies specifically reporting the phenotypic or genetic correlations between CC DTI metrics and WMLs.

In this study, we estimate the relative influence of genetic and environmental factors on DTI measures for the entire CC and for five parcellated regions using the method of Chao et al., [39] in a community-dwelling sample of older adult twins. Examination of five regions of the CC based on anatomical and cortical connections will enable a hitherto more detailed examination of heritability than previous studies. Additionally, in contrast to the study of Pfefferbaum et al., [31] our sample contains both women and men aged 65 and above. In an extension of this, we aimed to determine whether there are common genetic influences across various DTI measures for whole CC and with WMLs, a marker of WM atrophy.

Methods

A. Ethics statement

The study was approved by the Australian Twin Registry, University of New South Wales, University of Melbourne, Queensland Institute of Medical Research and the South Eastern Sydney and Illawarra Area Health Service and written informed consent provided by all participants. Participant's information was de-identified and anonymized prior to analysis.

B. Participants

The current study is comprised of 142 twin pairs (MZ male=29 pairs; MZ female=50 pairs; DZ male=8 pairs; DZ female =33 pairs, DZ mixed =22 pairs) drawn from the longitudinal Older Australian Twin Study (OATS) with available brain imaging data. The mean age of the sample used in this study was 69.82 (+/- 4.76) years with ages ranging from 65 to 85. All participants were Caucasian. In the current analysis, individuals with a consensus diagnosis of dementia were also excluded.

Briefly, OATS recruited twins aged 65 years and above who were registered with the Australian Twin Registry and through recruitment drives across the three eastern states of Australia – New South Wales, Queensland and Victoria. Other inclusion criteria were ability to complete questionnaires in English and having a consenting co-twin. Individuals were excluded if they were diagnosed with any progressive malignancy or other life threatening illness or acute psychiatric disorder. The study was approved by the relevant ethics committees and written informed consent provided by all participants. The full details of the study have been published elsewhere [49]. The zygosity of the sample was assessed based on identity by descent using available genome-wide genotyping data along with self-report data [50].

Participants completed an extensive face-to-face interview, which included demographic, medical and health information. Data on alcohol consumption, tobacco smoking and diabetes were obtained by self-report questionnaires [49]. Fasting peripheral blood samples were obtained and assessed for total cholesterol (using a Beckman LX20 Analyser) and glucose levels (glucose oxidase method, Beckman Coulter, Fullerton, CA). Individuals whose fasting blood glucose level was ≥ 7 mmol/L or had been diagnosed by a medical practitioner as diabetic and were currently on a diabetic diet, hypoglycaemic tablets or insulin were categorised as diabetic. Two seated readings of systolic and diastolic blood pressure (BP) were obtained by the interviewer and averaged. For current smoking status, individuals were classified as either a current smoker or not. Daily alcohol consumption was based on the frequency of drinking and number of drinks (10 g alcohol) consumed on typical drinking days. Participants were classified into two categories: (i) ≤ 1 drink/day; (ii) > 1 drink/day. For handedness, individuals were categorised either as right-handed or not, based on a series of questions regarding which hand they used for various daily activities. As there

were very few left handed and mixed individuals in the sample, we combined them as non-right handed for our analysis (N=18).

C. Brain MRI Scanning

MRI data were obtained on three 1.5 Tesla scanners and a 3 Tesla scanner owing to the multi-site nature of this study. Co-twins were imaged on the same scanner. We used Siemens Magnetom Avanto and Sonata scanners (Siemens Medical Solutions, Malvern PA, USA) with similar years of manufacture and upgrade in centres 2 (Victoria - 97 participants) and 3 (Queensland- 79 participants), respectively. In centre 1 (New South Wales), we initially used a 1.5 T Philips Gyroscan scanner (Philips Medical Systems, Best, Netherlands) (83 participants) and subsequently a 3 Tesla Philips Achieva Quasar Dual scanner (25 participants). The acquisition protocols and parameters were tested and matched between the centres through standardization of spatial resolution and slice thickness, using a 3D phantom to correct geometric distortions and using five volunteers who were scanned on the four scanners [49]. Twin pairs were scanned on the same day or temporally very close to each other (<few weeks).

Diffusion weighted MRIs (DWI) scans were used for computing the diffusion tensor imaging (DTI) measures. DWI sequences were performed using a similar protocol for the 1.5 Tesla scanners in the three centres. To increase the signal-to-noise ratio (SNR), all of the subjects were scanned twice for DWI sequences in the same MRI session. A single-shot echo-planar imaging (EPI) sequence (TR=12729 ms, TE=76 ms) was used. Diffusion sensitizing gradients were applied along 32 non-collinear directions ($b_1=800 \text{ s/mm}^2$), together with a non-diffusion-weighted acquisition b_0 . For each DWI scan, 55 axial slices were collected. The field of view was 240 mmx240 mmx137.5 mm with acquisition matrix 96×96 , and slice thickness 2.5 mm with no gap between the slices, yielding 2.5 mm^3 voxels of isotropic sizes. Two extra non-diffusion-weighted (b_0) EPIs were separately acquired and then combined with DWI scans for higher SNR. TR=7115 ms and TE=70 ms and $b_1=1000 \text{ s/mm}^2$ were used for the 3 Tesla Philips Achieva Quasar Dual scanner at Centre 1 while the other DWI parameters were the same.

We used T2-weighted fluid attenuated inversion recovery (FLAIR) and 3D T1-weighted MRIs scans for the computation of white matter lesion (WMLs) volumes. 3D T1-weighted volumetric sequence was performed using a similar protocol in the three centres with in-plane resolution= $1 \times 1 \text{ mm}$, slice thickness=1.5 mm, slice number=144, TR=1530 ms, TE=3.24 ms, TI (Inversion time)=780 ms, and flip angle=8. Two T1-3D scans were acquired for each participant for an increased SNR. FLAIR scans main acquisition parameters were: TR/TE=10000/120 ms, inversion delay=2500 ms, in-plane resolution $0.898 \times 0.899 \text{ mm}^2$, slice thickness=3.0 mm, with 50 axial slices.

D. DTI Processing

The DTI data were pre-processed using FMRIB's Software Library (FSL) version 5.0 [51, 52], which included three main steps. Firstly, eddy current correction, which includes correction of DTI images due to head distortions and for different gradient directions; secondly, brain extraction, which includes the deletion of non-brain tissue, using BET (Brain Extraction Tool); and thirdly, fitting tensors using the DTIfit program, which includes the process of fitting the diffusion tensor model across each voxel of the pre-processed DTI data to derive anisotropic (FA) and diffusivity (MD, RD and AD) images. These images were then checked individually for any artefacts or missing slices. Any samples that failed quality control checks were removed from the analysis.

E. Tracing and parcellation of corpus callosum

A semi-automated method of tracing and parcellation of the CC was performed using Analyze version 11.0 (<http://www.analyzedirect.com/>) by a trained researcher who was blinded to family relationship. Initially, the pre-processed DTI images were adjusted to note the mid-sagittal slice number using volume render and fly tools. The auto-trace tool was used to trace whole CC in the mid-sagittal slice of FA images (Fig. 1). The traced CC was then parcellated into five vertical partitions (A–E) from anterior to posterior, as proposed by Chao et al., [39] using the grid divider tool (Fig. 2): A - frontal regions; B - pre motor & supplementary motor; C - motor; D - sensory; and E - parietal, temporal & occipital. The same object maps were loaded on MD, RD and AD images to obtain the respective DTI measures.

Tracing and parcellation were done individually on both images (i.e. scan 1 and 2 for each participant). The two sets of data were significantly correlated ($r > 0.8$, $p < 0.05$). The four DTI metrics were calculated using the three eigen vectors extracted from the DTI images. The mathematical formulae are shown in [S1 File](#) and show that all of the metrics are related and not independent. FA and MD values are derived from all three eigen vectors ($\lambda_1, \lambda_2, \lambda_3$), whilst RD is calculated from the average of two eigen vectors (λ_2 and λ_3) whilst λ_1 is taken as AD. The two sets of data (scans 1 & 2) were highly correlated ($r \geq 0.85$). Here, we report the heritability results based on the averages of the two scans. Additional analyses of the individual scans are presented in [S1 File](#).

F. Measurement of WMLs

WMLs were delineated from FLAIR and 3D T1-weighted structural scans using an automated pipeline described in detail previously [44, 53]. Briefly, the automatic quantification of WMLs was carried out in the following steps: 1) co-registration of each participant's FLAIR images to their corresponding T1-weighted structural images; 2) segmentation of T1-weighted structural images into three separate tissue components, i.e. grey matter, white matter and cerebrospinal fluid; 3) removal of non-brain tissue from both T1-weighted and co-registered FLAIR

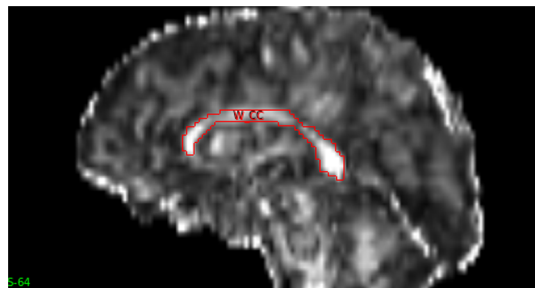


Fig. 1. Mid- sagittal slice showing tracing of the whole corpus callosum.

doi:10.1371/journal.pone.0113181.g001

images using a brain mask (computer generated, which is used to discriminate between brain from non-brain tissue) transformed from the average mask originally defined in the Talairach space (a 3-dimensional atlas of the brain); 4) inverting the spatial normalization transformation to produce the brain masks and WM probability maps in the individual imaging space for the WMLs detection and non-brain tissue removal; 5) intensity correction of both FLAIR and T1-weighted images after the removal of non-brain tissues and then 6) segmentation of WMLs using FLAIR scans.

G. Statistical analysis

The twin method was used to study the influence of genetic and environmental factors on a particular trait. Monozygotic (MZ) twins share all genes whereas dizygotic (DZ) twins share only half of their genes. By comparing the similarity between the identical and non-identical twin pairs for a particular trait, the effect of genetic, shared and non-shared factors can be estimated. We calculated heritability of the four DTI measures (FA, MD, RD and AD) across whole CC and its five sub regions as described below.

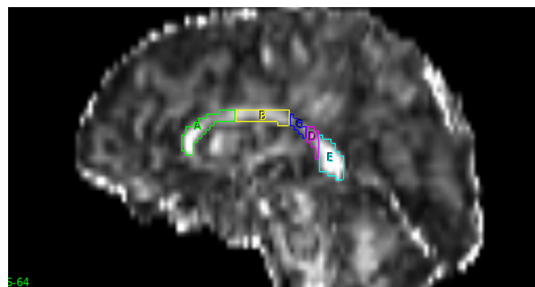


Fig. 2. Mid- sagittal slice showing the divisions of corpus callosum into 5 regions anterior to posterior (A–E) using the parcellation method of Chao et al. [39].

doi:10.1371/journal.pone.0113181.g002

Covariates

Age and scanner were significantly associated with the four DTI measures of whole CC ($p \leq 0.05$). Sex was significantly correlated with MD, AD and RD of whole CC ($p \leq 0.05$), but not FA ($p > 0.05$). Handedness was significantly associated with MD and RD of whole CC ($p \leq 0.05$) but not with whole CC FA ($p > 0.05$). Previous studies have identified risk factors for the integrity of WM across various regions of brain, which include hypertension, serum cholesterol [54–56], alcohol consumption [57], tobacco smoking [58] and diabetes [59, 60]. Of these potential confounders, only diastolic and systolic BP were significantly correlated with FA of the whole CC ($p \leq 0.05$). The other risk factors - total cholesterol, diabetes, alcohol consumption and smoking status - were not significantly associated with any of the DTI measures ($p > 0.05$). For the region-wise analysis of the CC sub regions, there was no specific pattern of association (see S1a Table and S1b Table in [S1 File](#)). To be consistent across analyses the following were used as covariates: age, sex, scanner, handedness, diastolic and systolic BP.

Heritability and genetic correlations

To estimate heritability and genetic correlations, the SOLAR (Sequential Oligogenic Linkage Analysis Routines) software package was used, which is based on the variance components method (<http://solar.txbiomedgenetics.org/>) [61]. The variance components model used here for heritability estimation includes only the genetic and environmental variance components. The shared environmental variance can be measured by adding an additional component of variance to the model. However, under the twin design, a very large sample is required to distinguish between those two models [62]. Since the shared environment component was not significant in our sample in other neuroimaging analyses, we therefore have used only the genetic and environment components for consistency [similar to 63]. Multiple traits can be analysed by extending the variance component model [64–66]. Heritability was also estimated separately for women ($N=166$) but not for men due to the relatively small sample size ($N=74$) and the imbalance between the number of MZ and DZ pairs ($\sim 4:1$).

Bivariate genetic correlations were assessed between (i) whole CC DTI metrics and (ii) whole CC DTI measures and total WML burden. Analyses were undertaken controlling for the covariates listed above.

Results

The demographic details of the sample are shown in [Table 1](#). There were more females (66.19%) than males. There was no significant difference between MZ and DZ pairs for all relevant variables ($p > 0.5$) including age ($p = 0.79$), sex ($p = 0.82$) and handedness ($p = 0.88$). The entire sample was mainly right-handed (89.75%), nearly one-third of the sample were current smokers (29.07%) and less than 14% were diabetic. The descriptive statistics of the DTI measures for the whole CC and

Table 1. Demographics and Characteristics of the Twin Sample.

	Total sample	MZ	DZ	p-values
N	284	158	126	
Age M (SD) yrs	69.82 (4.76)	69.92 (4.97)	69.69 (4.51)	0.79
Age Min/Max yrs	65/85	65/83	65/85	-
Sex - Female, N	188	100	88	0.39
Right-handed, N	254	140	114	0.87
Current smokers, N	82	50	32	0.40
Diabetic, N	32	21	11	0.23
Alcohol consumption >1 drink per day, N	66	43	23	0.20
Cholesterol (mmol/L) mean (SD)	5.20 (1.05)	5.10 (1.04)	5.33 (1.06)	0.58
Systolic mean (SD)	138.17 (18.15)	137.84 (18.92)	138.57 (17.21)	0.79
Diastolic mean (SD)	80.77 (10.35)	79.77 (9.95)	82.00 (10.75)	0.14
Total white matter lesions (mm ³)	6688.04 (7997.89)	6513.22 (7977.05)	6907.26 (8050.41)	0.12

Notes: MZ – monozygotic twins; DZ- Dizygotic twins; M –mean; SD – standard deviation.

doi:10.1371/journal.pone.0113181.t001

its sub- regions are shown in [Table 2](#). Total WMLs were significantly correlated with all the DTI metrics across the whole CC.

A. Heritability analysis

Intra-class correlations (ICC) estimated for MZ and DZ twin groups (95% CI) for whole CC DTI measures are shown in [Table 3](#). Since data was acquired and averaged from two separate scans of each individual, ICCs were also calculated for the major measures for the whole CC for comparison for each scan (see S2a Table and S2b Table in [S1 File](#)). Although the values for each scan differ slightly, the estimates and resulting heritability values were similar (see S3a Table and S3b Table in [S1 File](#)). The heritability estimates of the four DTI measures for whole CC and its five sub regions from anterior to posterior (A–E), are shown in [Table 4](#). For whole CC, moderate heritability was observed for all the four measures, FA, MD, RD and AD ($h^2=0.37-0.56$). For the region-wise analysis, similar to the entire CC, FA, MD and RD are heritable. However, AD is heritable only in the anterior CC (region A).

Significant heritability for women was observed for all four DTI measures ranging from 0.39–0.68 for the whole CC (see S4 Table in [S1 File](#), N=50 female MZ pairs and 33 DZ pairs).

B. Genetic correlation analysis

Bivariate genetic correlation analysis was performed for the whole CC between the four DTI measures [[Table 5](#)] and separately for each scan (see S5a Table and S5b Table in [S1 File](#)). In general, significant genetic correlations were observed between FA, MD, RD and AD. However, AD did not show a significant correlation with FA. FA shared around 11% ($\rho_g=-0.34$) and 51% ($\rho_g=-0.72$)

Table 2. Descriptive Statistics for the DTI measures.

CC Region	FA		MD (mm ² /s)		RD (mm ² /s)		AD (mm ² /s)	
	Mean	SD	Mean	SD	Mean	SD	Mean	SD
Whole CC	5.42×10^{-1}	4.8×10^{-2}	1.06×10^{-3}	1.3×10^{-4}	0.73×10^{-3}	1.1×10^{-4}	0.31×10^{-2}	7.5×10^{-4}
A ^a	5.13×10^{-1}	5.1×10^{-2}	1.08×10^{-3}	1.5×10^{-4}	0.77×10^{-3}	1.3×10^{-4}	0.30×10^{-2}	7.6×10^{-4}
B ^a	5.07×10^{-1}	5.6×10^{-2}	1.07×10^{-3}	1.4×10^{-4}	0.77×10^{-3}	1.3×10^{-4}	0.31×10^{-2}	8.0×10^{-4}
C ^a	4.63×10^{-1}	7.2×10^{-2}	1.18×10^{-3}	1.7×10^{-4}	0.88×10^{-3}	1.7×10^{-4}	0.32×10^{-2}	7.9×10^{-4}
D ^a	5.27×10^{-1}	7.3×10^{-2}	1.12×10^{-3}	1.6×10^{-4}	0.78×10^{-3}	1.6×10^{-4}	0.32×10^{-2}	8.1×10^{-4}
E ^a	6.21×10^{-1}	5.7×10^{-2}	0.99×10^{-3}	1.4×10^{-4}	0.62×10^{-3}	1.1×10^{-4}	0.31×10^{-2}	8.0×10^{-4}

Notes: FA – Fractional anisotropy; MD- Mean diffusivity; RD- Radial diffusivity; AD – Axial diffusivity; SD – standard deviation; CC – corpus callosum. The means are calculated considering all the voxels within that subregion^a.

doi:10.1371/journal.pone.0113181.t002

common genetic variance with MD and RD respectively. The negative sign of the correlation coefficient indicates opposing effects of the shared genetic factors on the measures, i.e. there are some shared genetic factors that are associated with an increase in FA and a decrease in MD or RD [32]. MD shared 85% of common genetic variance ($\rho_g=0.92$) with RD and 77% of common genetic variance ($\rho_g=0.88$) with AD in the same direction. Similarly RD and AD shared 37% common genetic variance ($\rho_g=0.61$).

High heritability was observed for total brain WMLs ($h^2=0.73$, $SE=0.051$, $p=3.03 \times 10^{-15}$). Bivariate genetic correlation analysis of the four DTI measures of the whole CC with total brain WMLs showed significant correlations for WMLs with all four DTI CC measures [Table 5]. Total brain WMLs shared 5% common genetic variance with FA with an inverse correlation observed ($\rho_g=-0.23$), indicating an opposing effect. On the other hand, positive genetic correlations were also observed with total brain WMLs sharing 19% common genetic variance with MD ($\rho_g=0.44$), 17% with RD ($\rho_g=0.42$) and 16% with AD ($\rho_g=0.40$).

Discussion

Our study of community-dwelling older adult twins aimed to estimate the role of genetic factors on the microstructure of the CC and its five sub regions using DTI.

Table 3. Intra-class correlations (ICC) estimates for MZ and DZ twin groups for whole CC DTI measures.

Whole CC	MZ ICC (95% C.I.)	DZ ICC (95% C.I.)
FA	0.62 (0.46–0.74)	0.39 (0.15–0.58)
MD	0.75 (0.63–0.83)	0.63 (0.45–0.76)
RD	0.65 (0.50–0.76)	0.46 (0.24–0.63)
AD	0.67 (0.53–0.78)	0.73 (0.59–0.83)

Notes: MZ – monozygotic twins; DZ- Dizygotic twins; FA – Fractional anisotropy; MD- Mean diffusivity; RD- radial diffusivity; AD – Axial diffusivity; ICC- Intra-class correlations.

doi:10.1371/journal.pone.0113181.t003

Table 4. Heritability estimates for Whole CC and its five sub-regions [A-E] for the four DTI measures.

CC Region	FA		MD		RD		AD	
	$h^2 \pm SE$	p-value	$h^2 \pm SE$	p-value	$h^2 \pm SE$	p-value	$h^2 \pm SE$	p-value
Whole CC	0.56 ± 0.07	$2.89 \times 10^{-10*}$	0.52 ± 0.08	$0.30 \times 10^{-6*}$	0.49 ± 0.08	$0.20 \times 10^{-6*}$	0.37 ± 0.09	$8.15 \times 10^{-5*}$
A	0.54 ± 0.07	$2.52 \times 10^{-9*}$	0.46 ± 0.09	$1.57 \times 10^{-5*}$	0.44 ± 0.09	$1.56 \times 10^{-5*}$	0.26 ± 0.10	0.08×10^{-1}
B	0.44 ± 0.08	$0.90 \times 10^{-6*}$	0.44 ± 0.09	$2.39 \times 10^{-5*}$	0.48 ± 0.09	$0.50 \times 10^{-6*}$	0.15 ± 0.09	0.05
C	0.34 ± 0.08	$2.18 \times 10^{-4*}$	0.36 ± 0.09	$1.38 \times 10^{-4*}$	0.39 ± 0.08	$2.19 \times 10^{-5*}$	0.07 ± 0.10	0.24
D	0.32 ± 0.08	$2.27 \times 10^{-4*}$	0.35 ± 0.08	$0.85 \times 10^{-4*}$	0.38 ± 0.08	$1.81 \times 10^{-5*}$	0.10 ± 0.10	0.16
E	0.49 ± 0.07	$4.15 \times 10^{-8*}$	0.40 ± 0.09	$2.65 \times 10^{-5*}$	0.40 ± 0.08	$5.30 \times 10^{-6*}$	0.15 ± 0.10	0.07

*Values are significant at $p < .0001$.

Notes: FA – Fractional anisotropy; MD- Mean diffusivity; RD- radial diffusivity; AD – Axial diffusivity; h^2 - heritability estimate; SE – standard error.

doi:10.1371/journal.pone.0113181.t004

In addition, we estimated the genetic correlations between whole CC DTI measures and with WMLs.

The heritability analysis indicated that all four DTI measures (FA, MD, RD and AD) for whole CC are moderately heritable. Our results are in agreement with the results of previous studies of older adults where FA and RD were heritable. In general, we also observed AD to be heritable in older individuals, which is contrary to the study by Kochunov et al. [32]. Differences between the two studies may explain the discrepancy in results. Here, we examined older twins only, whilst Kochunov et al. examined CC across the lifespan in a family study. Moreover, these prior studies did not examine the heritability of MD; we found MD to have moderate heritability [31, 32].

Our results vary from a previous study [31], which reported higher genetic contribution for the FA in the posterior CC (splenium h^2 - 67%) than the anterior CC (genu h^2 -49%). We did not observe such high heritability in the posterior regions of the CC. This may be due to differences in methods of tracing and

Table 5. Genetic (upper matrix) and environmental correlations (lower matrix) of whole CC DTI measures and total WMLs.

	FA ($\rho_g \pm SE$) [p]	MD ($\rho_g \pm SE$) [p]	RD ($\rho_g \pm SE$) [p]	AD ($\rho_g \pm SE$) [p]	WMLs ($\rho_g \pm SE$) [p]
FA ($\rho_e \pm SE$) [p]	1	-0.34 ± 0.11 [0.01]*	-0.72 ± 0.07 [2.74×10^{-6}]*	0.08 ± 0.15 [0.58]	-0.23 ± 0.11 [0.04]
MD ($\rho_e \pm SE$) [p]	-0.61 ± 0.07 [9.78×10^{-10}]*	1	0.92 ± 0.02 [1.15×10^{-6}]*	0.88 ± 0.07 [3.17×10^{-6}]*	0.44 ± 0.13 [0.6×10^{-3}]*
RD ($\rho_e \pm SE$) [p]	-0.79 ± 0.04 [2.01×10^{-22}]*	0.90 ± 0.02 [2.01×10^{-53}]*	1	0.61 ± 0.12 [0.31×10^{-3}]*	0.42 ± 0.13 [0.89×10^{-3}]*
AD ($\rho_e \pm SE$) [p]	0.10 ± 0.10 [0.29]	0.52 ± 0.07 [1.67×10^{-9}]*	0.24 ± 0.09 [0.01]	1	0.40 ± 0.13 [0.32×10^{-2}]*
WMLs ($\rho_e \pm SE$) [p]	0.03 ± 0.11 [0.79]	-0.13 ± 0.11 [0.26]	-0.109 ± 0.11 [0.39]	0.03 ± 0.10 [0.76]	1

*Values are significant at $p < 0.01$.

Notes: FA – Fractional anisotropy; MD- Mean diffusivity; RD- radial diffusivity; AD – Axial diffusivity; WMLs – White matter lesions; ρ_g – genetic correlation coefficient; ρ_e - environmental correlations; SE – standard error.

doi:10.1371/journal.pone.0113181.t005

parcellation, and the fact our sample is slightly younger (mean age of our sample 69.8 years vs 76 years) and includes both sexes. However, our results are similar to the results of Kochunov et al., [32], which used an extended family sample.

Genetic factors account for approximately 56% of the variance in CC FA, which may be sensitive to levels of myelination, axonal density and its diameter [6–10]. Similarly for MD, RD and AD, genetic factors contribute about 50% of the observed variability. Likewise, region wise analyses for the heritability of DTI measures across CC also indicated that heritability values for FA, MD and RD showed moderate heritability (31–54%). Moderate heritability was observed for AD but only in the anterior CC (region A).

We studied bivariate genetic correlation analysis between the DTI metrics for the whole CC. In our analysis, MD-RD shared the highest common genetic variance (84%), followed by MD- AD (77%), FA - RD (52%), RD - AD (37%) and FA – MD (11%). The relationship between MD and RD may be explained by the strong mathematical relationship between these two measures. In the DTI analysis, the magnitude and direction of maximum and minimum water diffusion at each voxel are quantified as three Eigen values at each voxel. MD being the average of the three Eigen values provides the measure of rate of water diffusion whereas RD, which is the average of the second and third Eigen values, is a measure of transverse diffusion. AD is the largest of the three Eigen values and is a measure of the rate of diffusion along the primary axis. As discussed previously, different DTI measures may be sensitive to different aspects of WM integrity and a better understanding of the relationships between these DTI measures may help to understand the underlying changes occurring in axons and myelin in older individuals. However, the relationship between the DTI measures and the tissue microstructural properties are not yet completely understood [67, 68].

Bivariate genetic correlation analysis of total brain WMLs with whole CC DTI metrics also indicated some common genetic factors between them, with the highest shared common genetic variance observed with MD and RD. The significant genetic correlations observed may reflect shared genetic variance that contributes to common pathological processes leading to age-related WM pathology. WMLs are usually regarded as markers of small vessel disease [69] although their pathology is not completely understood [45]. However, the CC is less affected by small vessel disease [70]. Therefore, the common genetic factors between these measures, as reported in our results, may possibly indicate some other genetic factors for WMLs that are independent of small vessel disease.

This study has a few limitations. Firstly, the DTI metrics were for CC only, while the measures of WMLs, which are not generally observed in CC, were for the total brain. Another limitation is that the MRI scans were collected across three states and used four scanners. However, this is a relatively common issue in multicenter DTI studies and we scanned the twin pairs on the same scanner and also adjusted for the scanner in our analyses. Secondly, we did not explore the shared genetic variance between WM integrity of the CC and its connected cortical regions, as measured by cortical thickness, which may assist in the clarification of the genetic basis of the connectivity of CC. Thirdly, we performed

a cross-sectional study. It would be of interest to examine the heritability of longitudinal change in the integrity of CC. And lastly, we note that the “environment” component calculated in heritability estimates not only includes environmental variation but also any measurement error in the phenotypes measured.

In conclusion, we observed that in general, the CC microstructure as measured by DTI is under moderate genetic control in older adults. All the CC DTI metrics FA, MD, RD and AD showed significant heritability for whole CC. These measures may serve as useful phenotypes to identify specific genetic variants associated with CC integrity in older individuals. Additionally, we observed some common genetic factors between whole CC DTI metrics and also with CC DTI measures and WMLs, which may lead to further investigations to uncover common genes contributing to age-related changes in WM microstructure in the future.

Supporting Information

S1 File. This file contains S1 Table–S5 Table. S1a Table, Summary of covariate results used in the variance components model for whole CC and its sub regions (FA & MD). S1b Table, Summary of covariate results used in the variance components model for whole CC and its sub regions (RD & AD). S2a Table, Intra-class correlations (ICC) estimates for MZ and DZ twin groups for whole CC DTI measures for Scan 1. S2b Table, Intra-class correlations (ICC) estimates for MZ and DZ twin groups for whole CC DTI measures for Scan 2. S3a Table, Heritability estimates for Whole CC and its five sub-regions [A–E] for the four DTI measures for scan 1. S3b Table, Heritability estimates for Whole CC and its five sub-regions [A–E] for the four DTI measures for scan 2. S4 Table, Heritability estimates for the four DTI measures of whole CC in females. S5a Table, Genetic (upper matrix) and environmental correlations (lower matrix) of whole CC DTI measures and total WMLs for scan 1. S5b Table, Genetic (upper matrix) and environmental correlations (lower matrix) of whole CC DTI measures and total WMLs for scan 2.

[doi:10.1371/journal.pone.0113181.s001](https://doi.org/10.1371/journal.pone.0113181.s001) (DOC)

Acknowledgments

We would like to thank the OATS participants, their supporters and respective Research Teams.

Author Contributions

Conceived and designed the experiments: KAM AT WW PSS. Performed the experiments: SCK. Analyzed the data: SCK KAM AT. Contributed reagents/materials/analysis tools: LZ WW. Wrote the paper: SCK KAM AT WW.

Contributed to the conception and design of the work: SCK KAM AT LZ PRS JBJK DA MJW JNT WW PSS. Contributed to acquisition of the data or analysis and interpretation of data: SCK KAM AT LZ PRS JBJK DA MJW JNT WW PSS. Contributed to drafting/revisions and give final approval of the version to be published: SCK KAM AT LZ PRS JBJK DA MJW JNT WW PSS. Agreed to be accountable for the work: SCK KAM AT LZ PRS JBJK DA MJW JNT WW PSS.

References

1. **Van der Knaap LJ, van der Ham IJ** (2011) How does the corpus callosum mediate interhemispheric transfer? A review. *Behavioural Brain Research* 223: 211–221.
2. **Aboitiz F, Scheibel AB, Fisher RS, Zaidel E** (1992) Fiber composition of the human corpus callosum. *Brain Research* 598: 143–153.
3. **Bloom JS, Hynd GW** (2005) The role of the corpus callosum in interhemispheric transfer of information: excitation or inhibition? *Neuropsychology Review* 15: 59–71.
4. **Basser PJ, Mattiello J, LeBihan D** (1994) MR diffusion tensor spectroscopy and imaging. *Biophysical Journal* 66: 259–267.
5. **Persson J, Nyberg L, Lind J, Larsson A, Nilsson LG, et al.** (2006) Structure-function correlates of cognitive decline in aging. *Cerebral Cortex* 16: 907–915.
6. **Bastin ME, Clayden JD, Pattie A, Gerrish IF, Wardlaw JM, et al.** (2009) Diffusion tensor and magnetization transfer MRI measurements of periventricular white matter hyperintensities in old age. *Neurobiology of Aging* 30: 125–136.
7. **Beaulieu C** (2002) The basis of anisotropic water diffusion in the nervous system - a technical review. *NMR in Biomedicine* 15: 435–455.
8. **Budde MD, Kim JH, Liang HF, Schmidt RE, Russell JH, et al.** (2007) Toward accurate diagnosis of white matter pathology using diffusion tensor imaging. *Magnetic resonance in medicine: Official Journal of the Society of Magnetic Resonance in Medicine/Society of Magnetic Resonance in Medicine* 57: 688–695.
9. **Song SK, Sun SW, Ju WK, Lin SJ, Cross AH, et al.** (2003) Diffusion tensor imaging detects and differentiates axon and myelin degeneration in mouse optic nerve after retinal ischemia. *NeuroImage* 20: 1714–1722.
10. **Song SK, Yoshino J, Le TQ, Lin SJ, Sun SW, et al.** (2005) Demyelination increases radial diffusivity in corpus callosum of mouse brain. *NeuroImage* 26: 132–140.
11. **Schulte T, Sullivan EV, Muller-Oehring EM, Adalsteinsson E, Pfefferbaum A** (2005) Corpus callosal microstructural integrity influences interhemispheric processing: a diffusion tensor imaging study. *Cerebral Cortex* 15: 1384–1392.
12. **Luders E, Thompson PM, Toga AW** (2010) The development of the corpus callosum in the healthy human brain. *The Journal of Neuroscience* 30: 10985–10990.
13. **Salat D, Ward A, Kaye JA, Janowsky JS** (1997) Sex differences in the corpus callosum with aging. *Neurobiology of Aging* 18: 191–197.
14. **Takeda S, Hirashima Y, Ikeda H, Yamamoto H, Sugino M, et al.** (2003) Determination of indices of the corpus callosum associated with normal aging in Japanese individuals. *Neuroradiology* 45: 513–518.
15. **Ota M, Obata T, Akine Y, Ito H, Ikehira H, et al.** (2006) Age-related degeneration of corpus callosum measured with diffusion tensor imaging. *NeuroImage* 31: 1445–1452.
16. **Sullivan EV, Rohlfing T, Pfefferbaum A** (2010) Longitudinal study of callosal microstructure in the normal adult aging brain using quantitative DTI fiber tracking. *Developmental Neuropsychology* 35: 233–256.
17. **Fling BW, Chapekis M, Reuter-Lorenz PA, Anguera J, Bo J, et al.** (2011) Age differences in callosal contributions to cognitive processes. *Neuropsychologia* 49: 2564–2569.

18. **Ryberg C, Rostrup E, Paulson OB, Barkhof F, Scheltens P, et al.** (2011) Corpus callosum atrophy as a predictor of age-related cognitive and motor impairment: a 3-year follow-up of the LADIS study cohort. *Journal of the Neurological Sciences* 307: 100–105.
19. **Zahr NM, Rohlfing T, Pfefferbaum A, Sullivan EV** (2009) Problem solving, working memory, and motor correlates of association and commissural fiber bundles in normal aging: a quantitative fiber tracking study. *NeuroImage* 44: 1050–1062.
20. **Salami A, Eriksson J, Nilsson LG, Nyberg L** (2012) Age-related white matter microstructural differences partly mediate age-related decline in processing speed but not cognition. *Biochimica et Biophysica Acta* 1822: 408–415.
21. **Serbruyns L, Gooijers J, Caeyenberghs K, Meesen RL, Cuypers K, et al.** (2013) Bimanual motor deficits in older adults predicted by diffusion tensor imaging metrics of corpus callosum subregions. *Brain Structure & Function*.
22. **Di Paola M, Luders E, Di Iulio F, Cherubini A, Passafiume D, et al.** (2010) Callosal atrophy in mild cognitive impairment and Alzheimer's disease: different effects in different stages. *NeuroImage* 49: 141–149.
23. **Filippini N, Douaud G, Mackay CE, Knight S, Talbot K, et al.** (2010) Corpus callosum involvement is a consistent feature of amyotrophic lateral sclerosis. *Neurology* 75: 1645–1652.
24. **Wang PJ, Saykin AJ, Flashman LA, Wishart HA, Rabin LA, et al.** (2006) Regionally specific atrophy of the corpus callosum in AD, MCI and cognitive complaints. *Neurobiology of aging* 27: 1613–1617.
25. **Wiltshire K, Concha L, Gee M, Bouchard T, Beaulieu C, et al.** (2010) Corpus callosum and cingulum tractography in Parkinson's disease. *The Canadian Journal of Neurological Sciences* 37: 595–600.
26. **Alves GS, O'Dwyer L, Jurcoane A, Oertel-Knochel V, Knochel C, et al.** (2012) Different patterns of white matter degeneration using multiple diffusion indices and volumetric data in mild cognitive impairment and Alzheimer patients. *PLoS one* 7: e52859.
27. **Duffy SL, Paradise M, Hickie IB, Lewis SJ, Naismith SL, et al.** (2013) Cognitive impairment with and without depression history: an analysis of white matter microstructure. *Journal of Psychiatry & Neuroscience*: 38: 130079.
28. **Liu J, Yin C, Xia S, Jia L, Guo Y, et al.** (2013) White matter changes in patients with amnesic mild cognitive impairment detected by diffusion tensor imaging. *PLoS one* 8: e59440.
29. **Wang JH, Lv PY, Wang HB, Li ZL, Li N, et al.** (2013) Diffusion tensor imaging measures of normal appearing white matter in patients who are aging, or have amnesic mild cognitive impairment, or Alzheimer's disease. *Journal of Clinical Neuroscience* 20: 1089–1094.
30. **Kanchibhotla SC, Mather KA, Wen W, Schofield PR, Kwok JB, et al.** (2013) Genetics of ageing-related changes in brain white matter integrity - a review. *Ageing Research Reviews* 12: 391–401.
31. **Pfefferbaum A, Sullivan EV, Carmelli D** (2001) Genetic regulation of regional microstructure of the corpus callosum in late life. *Neuroreport* 12: 1677–1681.
32. **Kochunov P, Glahn DC, Lancaster JL, Winkler AM, Smith S, et al.** (2010) Genetics of microstructure of cerebral white matter using diffusion tensor imaging. *NeuroImage* 53: 1109–1116.
33. **Aboitiz F, Scheibel AB, Fisher RS, Zaidel E** (1992) Individual differences in brain asymmetries and fiber composition in the human corpus callosum. *Brain Research* 598: 154–161.
34. **Clarke JM, Zaidel E** (1994) Anatomical-behavioral relationships: corpus callosum morphometry and hemispheric specialization. *Behavioural Brain Research* 64: 185–202.
35. **Hasan KM, Kamali A, Kramer LA, Papnicolaou AC, Fletcher JM, et al.** (2008) Diffusion tensor quantification of the human midsagittal corpus callosum subdivisions across the lifespan. *Brain Research* 1227: 52–67.
36. **Witelson SF** (1989) Hand and sex differences in the isthmus and genu of the human corpus callosum. A postmortem morphological study. *Brain* 112 (Pt 3): 799–835.
37. **Stievenart JL, Iba-Zizen MT, Tourbah A, Lopez A, Thibierge M, et al.** (1997) Minimal surface: a useful paradigm to describe the deeper part of the corpus callosum? *Brain Research Bulletin* 44: 117–124.
38. **Weis S, Kimbacher M, Wenger E, Neuhold A** (1993) Morphometric analysis of the corpus callosum using MR: correlation of measurements with aging in healthy individuals. *AJNR American Journal of Neuroradiology* 14: 637–645.

39. **Chao YP, Cho KH, Yeh CH, Chou KH, Chen JH, et al.** (2009) Probabilistic topography of human corpus callosum using cytoarchitectural parcellation and high angular resolution diffusion imaging tractography. *Human Brain Mapping* 30: 3172–3187.
40. **Hofer S, Frahm J** (2006) Topography of the human corpus callosum revisited—comprehensive fiber tractography using diffusion tensor magnetic resonance imaging. *NeuroImage* 32: 989–994.
41. **Huang H, Zhang J, Jiang H, Wakana S, Poetscher L, et al.** (2005) DTI tractography based parcellation of white matter: application to the mid-sagittal morphology of corpus callosum. *NeuroImage* 26: 195–205.
42. **Park HJ, Kim JJ, Lee SK, Seok JH, Chun J, et al.** (2008) Corpus callosal connection mapping using cortical gray matter parcellation and DT-MRI. *Human Brain Mapping* 29: 503–516.
43. **Fazekas F** (1989) Magnetic resonance signal abnormalities in asymptomatic individuals: their incidence and functional correlates. *European Neurology* 29: 164–168.
44. **Wen W, Sachdev P** (2004) The topography of white matter hyperintensities on brain MRI in healthy 60- to 64-year-old individuals. *NeuroImage* 22: 144–154.
45. **Assareh A, Mather KA, Schofield PR, Kwok JB, Sachdev PS** (2011) The genetics of white matter lesions. *CNS Neuroscience & Therapeutics* 17: 525–540.
46. **de Groot M, Verhaaren BF, de Boer R, Klein S, Hofman A, et al.** (2013) Changes in normal-appearing white matter precede development of white matter lesions. *Stroke* 44: 1037–1042.
47. **Iverson GL, Hakulinen U, Waljas M, Dastidar P, Lange RT, et al.** (2011) To exclude or not to exclude: white matter hyperintensities in diffusion tensor imaging research. *Brain Injury* 25: 1325–1332.
48. **Lange RT, Shewchuk JR, Heran MK, Rauscher A, Jarrett M, et al.** (2013) To Exclude or Not To Exclude: Further Examination of the Influence of White Matter Hyperintensities in Diffusion Tensor Imaging Research. *Journal of Neurotrauma* 31(2): 198–205.
49. **Sachdev PS, Lammell A, Trollor JN, Lee T, Wright MJ, et al.** (2009) A comprehensive neuropsychiatric study of elderly twins: the Older Australian Twins Study. *Twin Research and Human Genetics* 12: 573–582.
50. **Batouli SA, Sachdev PS, Wen W, Wright MJ, Suo C, et al.** (2012) The heritability of brain metabolites on proton magnetic resonance spectroscopy in older individuals. *NeuroImage* 62: 281–289.
51. **Behrens TE, Woolrich MW, Jenkinson M, Johansen-Berg H, Nunes RG, et al.** (2003) Characterization and propagation of uncertainty in diffusion-weighted MR imaging. *Magnetic Resonance in Medicine* 50: 1077–1088.
52. **Jenkinson M, Beckmann CF, Behrens TE, Woolrich MW, Smith SM** (2012) FSL. *NeuroImage* 62: 782–790.
53. **Wen W, Sachdev PS, Li JJ, Chen X, Anstey KJ** (2009) White matter hyperintensities in the forties: their prevalence and topography in an epidemiological sample aged 44–48. *Human Brain Mapping* 30: 1155–1167.
54. **Williams VJ, Leritz EC, Shepel J, McGlinchey RE, Milberg WP, et al.** (2013) Interindividual variation in serum cholesterol is associated with regional white matter tissue integrity in older adults. *Human Brain Mapping* 34: 1826–1841.
55. **Burgmans S, van Boxtel M, Gronenschild E, Vuurman E, Hofman P, et al.** (2010) Multiple Indicators of Age-related Differences in Cerebral White Matter and the Modifying Effects of Hypertension. *NeuroImage* 49: 2083.
56. **Maillard P, Seshadri S, Beiser A, Himali JJ, Au R, et al.** (2012) Effects of systolic blood pressure on white-matter integrity in young adults in the Framingham Heart Study: a cross-sectional study. *Lancet Neurology* 11: 1039–1047.
57. **McQueeny T, Schweinsburg BC, Schweinsburg AD, Jacobus J, Bava S, et al.** (2009) Altered white matter integrity in adolescent binge drinkers. *Alcoholism, Clinical and Experimental Research* 33: 1278–1285.
58. **Hudkins M, O'Neill J, Tobias MC, Bartzokis G, London ED** (2012) Cigarette smoking and white matter microstructure. *Psychopharmacology* 221: 285–295.
59. **Antenor-Dorsey JA, Meyer E, Rutlin J, Perantie DC, White NH, et al.** (2013) White matter microstructural integrity in youth with type 1 diabetes. *Diabetes* 62: 581–589.

60. **Reijmer YD, Brundel M, de Bresser J, Kappelle LJ, Leemans A, et al.** (2013) Microstructural white matter abnormalities and cognitive functioning in type 2 diabetes: a diffusion tensor imaging study. *Diabetes Care* 36: 137–144.
61. **Almasy L, Blangero J** (1998) Multipoint quantitative-trait linkage analysis in general pedigrees. *American Journal of Human Genetics* 62: 1198–1211.
62. **Visscher PM, Gordon S, Neale MC** (2008) Power of the classical twin design revisited: II detection of common environmental variance. *Twin Research and Human Genetics* 11: 48–54.
63. **Jahanshad N, Kochunov PV, Sprooten E, Mandi RC, Nichols TE, et al.** (2013) Multi-site genetic analysis of diffusion images and voxelwise heritability analysis: a pilot project of the ENIGMA-DTI working group. *NeuroImage* 81: 455–469.
64. **Almasy L, Dyer TD, Blangero J** (1997) Bivariate quantitative trait linkage analysis: pleiotropy versus coincident linkages. *Genetic Epidemiology* 14: 953–958.
65. **Hopper JL, Mathews JD** (1982) Extensions to multivariate normal models for pedigree analysis. *Annals of Human Genetics* 46: 373–383.
66. **Williams JT, Van Eerdewegh P, Almasy L, Blangero J** (1999) Joint multipoint linkage analysis of multivariate qualitative and quantitative traits. I. Likelihood formulation and simulation results. *American Journal of Human Genetics* 65: 1134–1147.
67. **Alger JR** (2012) The diffusion tensor imaging toolbox. *J Neurosci* 32: 7418–7428.
68. **Seiler S, Cavalieri M, Schmidt R** (2012) Vascular cognitive impairment - An ill-defined concept with the need to define its vascular component. *J Neurol Sci* 22: 22.
69. **Fazekas F, Wardlaw JM** (2013) The origin of white matter lesions: a further piece to the puzzle. *Stroke* 44: 951–952.
70. **Srikanth V, Phan TG, Chen J, Beare R, Stapleton JM, et al.** (2010) The location of white matter lesions and gait—a voxel-based study. *Annals of Neurology* 67: 265–269.